Improvement of self-sufficiency for an innovative nearly zero energy building by photovoltaic generators

Improvement of Self-Sufficiency for an Innovative Nearly Zero Energy Building by Photovoltaic Generators

Paolo Di Leo, Filippo Spertino, Stefania Fichera, Gabriele Malgaroli, Alessandro Ratclif
Dipartimento Energia "Galileo Ferraris"
Politecnico di Torino
Corso Duca degli Abruzzi 24, Torino, Italy
paolo.dileo@polito.it, filippo.spertino@polito.it

***Abstract*—In the present work, a case study of an innovative nearly Zero Energy Building (nZEB) for academic purposes is investigated. In particular, its primary energy vector is electrical, i.e. a Photovoltaic (PV) generator is coupled with storage units and supplies the electrical loads and the thermal demand, which is converted into electrical by heat pumps. The system is designed to maximize the self-sufficiency and minimize the absorption from the grid. Moreover, the nZEB is equipped with sensors that are oriented to smart metering in order to monitor the energy exchange between the rooms of the building. An energy simulation is performed on a yearly basis, evaluating the size of the batteries, to reach the optimal compromise between benefits, in terms of self-sufficiency, and costs.**

***Index Terms*--grid absorption, nearly Zero Energy Building, photovoltaic generator, self-sufficiency, smart metering.**

I. Introduction

Nowadays, Renewable Energy Sources (RES) play an important role in producing significant share of electricity and reducing the emissions of carbon dioxide and other greenhouse gases. One of the most important RES is the Photovoltaic (PV) technology: indeed, it requires reduced installation and maintenance costs and it is the most suitable for urban integration thanks to the modularity of the structure and the limited installation spaces [1]. In this context, the concept of nearly Zero Energy Buildings (nZEBs) is fully framed. This term has been introduced by the European Commission with the Directive 2010/31/EU [2] and it defines appropriate measures, at national level, to increase the number of nZEBs. In particular, in a nZEB energy consumptions must be significantly covered by RES located on-site or nearby. Moreover, the European member states ensure that, by 31/12/2020, all new buildings will be nZEBs. Among the first, universities should take an active part in the nZEB frame, due to their relevant socio-economic impact [3-4]. Indeed, some universities already moved in this direction, focusing on possible retrofits to reduce the energy consumptions of existing academic buildings [5-7]. Samples of established buildings have been realized in University of Lleida (Spain), in Oberlin College (Ohio, USA) and in CSIRO Energy Centre (Newcastle, Australia). Other examples of nZEB schools and sustainable buildings for academic purposes are reported in [8]. In [9] the self-sufficiency ratio of residential buildings in Sweden is analyzed, focusing on the best battery technology for this purpose. Instead, in [10] the self-consumption and the self-sufficiency are discussed for a commercial building in Germany equipped with a battery storage system. Several studies, [11] and [12], based on domestic nZEBs, focus on self-sufficiency rate depending on battery size.

With respect to the above-mentioned research projects, this work designs and simulates a prototype of a prefabricated wooden nZEB for academic purposes. It will be built in the university campus of Politecnico di Torino. The building will be composed of four modular units and it will be used by students and professors of the university. The innovative feature of the present project is the multidisciplinary combination of architectural, electrical and thermal design, in order to achieve an optimal compromise between costs and benefits, in terms of self-sufficiency. The building is designed to be independent from the gas network and to reach the almost total autonomy from the electricity grid in terms of absorption. In particular, one goal will be to maximize self-sufficiency, reaching 100% independency, from the viewpoint of thermal and electrical energies, for most of the year. In this context, a proper design of a PV-storage system has been performed in order to satisfy the electrical consumptions and the thermal demand due to seasonal conditioning or heating [13]. Another innovative aspect of the project consists of the primary energy source: indeed, the loads will be mainly met by the PV-storage system. Moreover, the contemporaneity between loads and solar PV production is guaranteed, being this nZEB used not for residential but for academic purposes [10]. Furthermore, the project includes the installation of proper sensors, smart metering oriented, to monitor the demand and generation profiles. In future works, the electricity exchange between the units will be analyzed, i.e. the rooms of the nZEB considered as separate active users.

The paper is structured as follows: in Section II the design of the case study and the procedure to size the storage is described. Section III presents the estimation of the thermal and electrical loads of the building. In Section IV, the prediction of PV production, the storage model and the energy balance for the sizing calculation on a yearly base are reported. In Section V the results of the simulations are presented and the last section contains the conclusions.

II. THE SIMULATED SYSTEM

A. Description of the system

Regarding the architectural aspect, the building is made of eco-friendly materials as cork and wood, and it is divided in four units, each with an independent entrance. In particular, it is composed of two study rooms, where students can study and university employees can work during the day, a control room, where a continuous monitoring of the entire system is performed, and a technical room, where the energy conversion devices and the batteries are located. The generation is composed of the PV modules and the Battery Energy Storage System (BESS), both connected to the DC Bus. They are coupled with the DC/AC converters to feed the AC loads. The main goal of the system is to supply the loads by a PV generator, minimizing the absorption from the grid. Nevertheless, grid connection is performed as required by the DC-AC converters chosen for the project. The PV generator, the storage in discharge phase and the grid behave like generators. The block diagram of the system is shown in Fig. 1.

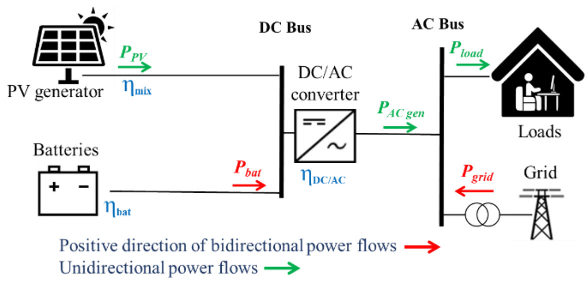

Figure 1. System block diagram.

The PV generator consists of mono-crystalline modules [14] with a rated power of 360 W and a very high efficiency of 22.2%. The panel specifications are provided at Standard Test Conditions (STC, with irradiance G_{STC}=1000 W/m^2, cell temperature T_{STC}=25°C and air mass AM=1.5). Moreover, the PV generator has a rated power of 8.64 kW and it is divided into four arrays located on the four sides of the roof, with the same rated power of 2.16 kW (i.e., six PV modules each section). This is the maximum power that can be installed to place the same number of modules on each side of the roof. Distances between the PV arrays are determined to minimize the mutual shading, during central sunlight hours in winter, according to [15].

PV modules face four perpendicular orientations (South-West, SW; North-East, NE; South-East, SE; North-West, NW) and each sub-array is coupled with a separate DC/AC converter and storage, except for the NE and SW sections that are connected to the same converter-storage system. In a second phase, the interconnection between the inverter-storage systems will be monitored (smart metering) to analyse the energy flows between units. In Table 1, the type of room according to the DC/AC converters, the orientation and the inclination, in terms of tilt angle β, of the PV modules is presented.

TABLE I. BUILDING ORGANIZATION

Type of room	**DC/AC converter**	**PV Orientation**	**PV Inclination**
Control Room	#1	SW	30°
Technical Room		NE	10°
Study Room #1	#2	SE	20°
Study Room #2	#3	NW	20°

In Fig. 2 the architectural layout of the building and the arrangement of the PV generator are shown.

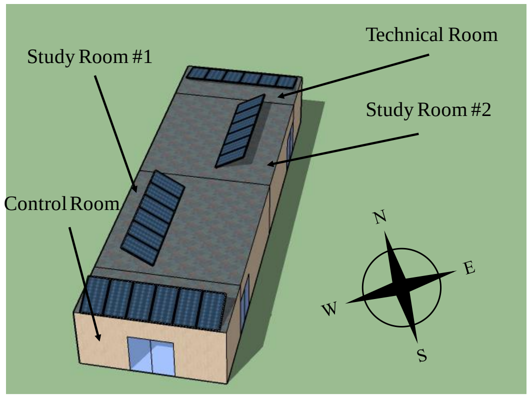

Figure 2. Layout of the building and arrangement of the PV generator.

The BESS consists of lithium-ion batteries and it is integrated into the DC/AC converter. Each inverter can manage storage capacities ranging from a minimum C_{min}=4 kWh to a maximum C_{max}=12 kWh. As previously mentioned, the building will be used as a study/meeting room: therefore, the electrical loads consist of Personal Computers (PCs), lighting devices, projectors, ventilation and heating systems (heat pump).

B. Sizing Procedure of the System

In the present project, the PV generator and the storage meet the global consumption of the loads, minimizing the energy absorbed from the grid [16]. In particular, the loads consist of a thermal demand, to obtain the desired temperature in the building, and electrical consumptions, related to the utilization of several devices. In order to size correctly the PV-storage system, the thermal and electrical consumptions of the building are estimated. Regarding the thermal demand, an energy balance is performed to evaluate the yearly energy required by a heat pump [17]. Then, the electrical consumptions of electronic devices such as PCs, lighting devices, and ventilation systems have been monitored for months in order to obtain representative load profiles. Moreover, a proper utilization profile of the devices is considered, according to the frequency of attendance of people using the study rooms, such as students or university employees.

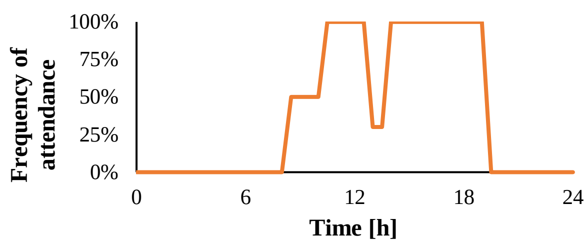

Figure 3. Frequency of attendance of the nZEB.

In Fig. 3, the predicted frequency of attendance of the building is reported.

Finally, several simulations are performed to evaluate the rating of the PV-storage system, in terms of batteries capacity, that permits to reach an adequate compromise between high self-sufficiency and low costs. In particular, the self-sufficiency parameter R_{suff} is defined according to the following formula:

$$R_{suff} = \frac{E_{pic}}{E_{load}} \qquad (1)$$

where E_{pic} is the amount of PV generation that is produced and, immediately, consumed, and E_{load} is the global demand of the building [18]. In Fig. 4 typical PV production and load profiles of the system in a clear sky day are presented. The green area identifies the energy supplied by PV generator, the red area indicates the energy absorbed from the grid and E_{waste} is the surplus energy that is wasted. R_{suff} is the ratio between the green area and the sum of the green and the red areas. The integration of a BESS will increase R_{suff}, reducing the energy absorbed from the grid (E_{grid}).

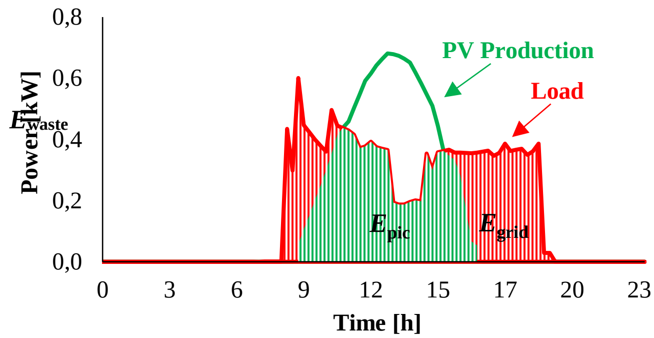

Figure 4. Typical PV generation and load profiles in clear sky conditions.

III. Estimation of Loads

A. Thermal loads

In order to evaluate the thermal demand of the building, a thermal energy balance is applied, taking into account the gains and the losses across the housing module. The system operates in two configurations: a heating configuration during winter and a cooling configuration in summer months [19]. In particular, during winter, the thermal demand is calculated according to equation (2):

$$Q_{h,nd} = (Q_{h,tr} + Q_{h,ve}) - \eta_{h,gn}(Q_{int} + Q_{sol}) \quad (2)$$

where $Q_{h,nd}$ is the thermal energy required by the system. Regarding the thermal losses, $Q_{h,tr}$ are losses due to transmission through the building envelope, $Q_{h,ve}$ are losses due to ventilation and replacement of air, that is necessary to maintain a high level of air quality. Q_{int} and Q_{sol} are thermal gains that take into account, respectively, the heat generated by internal sources such as humans, electrical devices etc., and the increase of internal temperature due to incident solar irradiance. However, only a quota of the gains is useful to reduce the heating demand, therefore, the gains are multiplied by a reduction factor $\eta_{H,gn}$, usually assumed between 0.7 and 0.8 for buildings with an efficient thermal response.

On the contrary, the thermal demand in summer is estimated according to equation (3):

$$Q_{c,nd} = (Q_{int} + Q_{sol}) - \eta_{c,gn}(Q_{c,tr} + Q_{c,ve}) \quad (3)$$

where $Q_{c,nd}$ is the thermal energy to be removed from the building. In summer configuration, Q_{int} and Q_{sol} are not gains but negative contributions for the cooling purpose. Regarding thermal gains, $Q_{c,tr}$ are the thermal flows exchanged with the ambient due to transmission through the wall and $Q_{c,ve}$ are cooling gains due to air replacement and infiltration. The parameter $\eta_{c,gn}$ is the reduction factor of the cooling gains.

B. Electrical loads

The building contains twenty-three computer workstations, each one with a dedicated Light Emitting Diode (LED) lamp and a PC. Moreover, every room is equipped with two ceiling lights, one projector and a ventilation system to provide the periodical replacement of internal air in the building.

Regarding the lighting devices, i.e. LED and ceiling lights, their consumption is supposed to be equal to, respectively, 9W and 23W when turned on. The consumption of the projector during the operation phase is equal to 190 W and the device is supposed to be operating, at maximum load, four hours per day. Several PCs are monitored for months in order to extract their typical load profiles: the maximum consumption of about 50 W is reached when the PCs are turned on. After few minutes, the devices absorb a steady-state power of about 30 W. During the stand-by configuration and when they are turned off, no power absorption occurs. In order to measure the absorbed power from such devices, a digital power meter is connected to the PCs, measuring the power with an uncertainty of ±0.3% of the full range.

IV. PV-Storage Models

A. Model of photovoltaic generator

Regarding the production of the PV generator, it is evaluated according to the single diode model [20]. First, the open-circuit voltage V_{oc} at cell temperature T_c is calculated with the following equation:

$$V_{oc} = V_{oc,ref} \cdot [1 + \beta_{Voc} \cdot (T_c - T_{STC})] \quad (4)$$

where β_{Voc} is the temperature coefficient of V_{oc} (assumed equal to -0.24 %/°C) and $V_{oc,ref}$ (69.5 V) is the open-circuit voltage of PV modules at STC conditions. Then, the current-voltage (I-V) characteristic curve of the generator is obtained calculating the current, at cell level and for each voltage value ranging from zero to V_{oc}, according to equation (5):

$$I = I_{ph} - I_0 \cdot \left(e^{\frac{q \cdot (V + R_S \cdot I)}{n \cdot k \cdot T_c}} - 1 \right) - \frac{(V + R_S \cdot I)}{R_{sh}} \qquad (5)$$

where I_{ph} is the photovoltaic current, I_0 is the dark saturation current (I_0=3.45·10^{-11}A), q is the electron charge (1.6·10^{-19} C), R_s is the series resistance of the cell (R_s=0.055 Ω), n is the non-ideality factor (n=1.5), k is the Boltzmann constant (1.38·10^{-23} J/K), and the shunt resistance of the cell is R_{sh} (210 Ω). Then, the AC power production $P_{AC\ gen}$ is obtained starting from maximum DC Power $P_{DC\ gen}$ at temperature T_c and irradiance G:

$$P_{AC\ gen} = P_{PV}(G, Tc) \cdot \eta_{PCU} \cdot \eta_{array} \qquad (7)$$

where η_{array} is an efficiency taking into account typical PV losses as exposed in [19], i.e. losses due to dirt, reflection from the glass, I-V mismatch, Joule effect in the cables. The parameter η_{PCU} incorporates losses due to Maximum Power Point (MPP) tracking, DC/DC and DC/AC conversion. In our analysis, it is assumed η_{PCU}=97% [15] and η_{array}=92% [20]. In order to estimate PV production, T_c is calculated according to:

$$T_c = T_a + \frac{NOCT - T_{a(NOCT)}}{G_{NOCT}} \cdot G \qquad (8)$$

Where T_a is the ambient temperature and $T_{a(NOCT)}$ is equal to 20°C. NOCT is the Nominal Operating Cell Temperature, that is the temperature of the modules in open circuit operation [21]. It is provided by the manufacturer (NOCT=46.8°C) and G_{NOCT}=800 W/m^2, that is the irradiance occurring at NOCT conditions.

However, the model does not take into account shading losses due to obstacles or adjacent PV modules. Therefore, PV production is also evaluated with the software System Advisor Model (SAM) [22]. It is a model that predicts the performance of grid-connected power systems: in particular, it uses the same above described model, providing the total AC generation $P_{AC,shad}$ with shading losses. The production profiles of the two models are compared in order to adjust the results of the single diode model.

B. Storage Model

The model used for the storage is an energy model that permits to calculate the State Of Charge (*SOC*) of the batteries at each time instant *t*, not requiring measurements of physical quantities [23]. In particular, the following equations are used:

$$SOC(t) = SOC(t-1) - \frac{P_{bat} \cdot \Delta t}{C_{Ebat}} \qquad P_{bat} > 0 \quad (9)$$

$$SOC(t) = SOC(t-1) - \frac{\eta_{bat} \cdot P_{bat} \cdot \Delta t}{C_{Ebat}} \quad P_{bat} < 0 \quad (10)$$

where SOC(t-1) is the state of charge at the previous time step, η_{bat} is the charging efficiency of the storage (it is assumed η_{bat}=96%), P_{bat} is the exchanged in the time step Δt and C_{Ebat} is the rated energy capacity as the product of rated voltage (V) and charge capacity (Ah). As described in Section II, during discharge phase (P_{bat}>0), the storage behaves like a generator and energy is provided to satisfy the loads. Vice versa, in charging phase, the batteries behave like loads and energy is absorbed by the storage.

The performance of the BESS can degrade [24] depending on several factors like not optimal charging patterns, overcharging, undercharging and abnormal cycling conditions caused by atypical charging temperature. In order to protect the storage from degradation, two limits are imposed. A power limit is imposed to avoid too high currents in the storage, i.e. P_{bat} cannot exceed a limit power $P_{bat,limit}$. Moreover, an energy limit avoids the complete discharge of the batteries. In particular, the storage always contains a minimum amount of energy that cannot satisfy the loads and the *SOC* cannot be lower than a minimum *SOC* value (SOC_{min}=5%). These limits are imposed according to the technical specification of the considered storage units.

C. Energy balance

The average power exchanged with the grid is calculated on a yearly basis with a time step Δt =15 minutes, according to (11):

$$P_{grid} = P_{load} - P_{PV} - P_{bat} \qquad (11)$$

where P_{grid} is the average power absorbed from the grid, P_{load} is the consumption, P_{PV} is the PV production and P_{batt} is the average power provided by the storage. In the present work, the simulations are performed with storage capacity ranging from 16 kWh to 36 kWh, with steps of 4 kWh.

V. RESULTS

As described in section III, PV production is calculated using both single diode model and the software SAM. The results of the two models have been compared to evaluate the shading effect due to obstacles and adjacent PV modules [25]. In particular, PV production, calculated with single diode model, is equal to 8660 kWh, while the software estimates a yearly PV production of 8878 kWh .

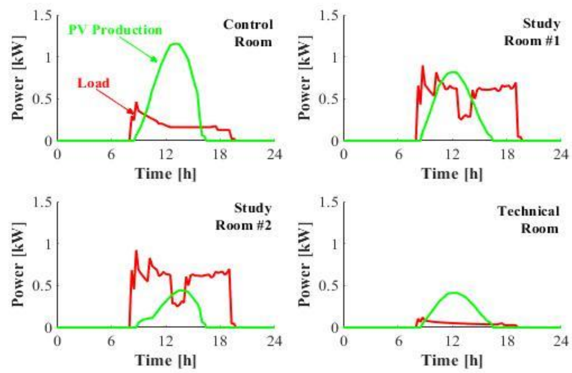

Figure 5. Production and load profiles of January 15th.

The difference between the two methods is about 2.5%, this means that the building is located in an optimal site, and that shading effect is not relevant in the present case study. Therefore, the results of the single diode model are used in the simulations to size the storage. The profiles of PV production and electrical loads for each section are presented in Fig. 5 and Fig. 6.

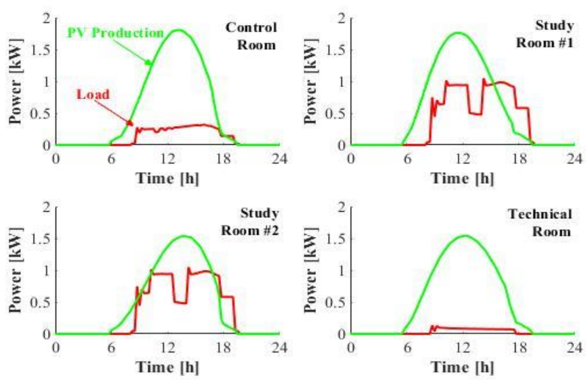

Figure 6. Production and load profiles of July 15th.

They refer to a typical winter day and a summer day in clear sky conditions, respectively, i.e. the incident irradiance on the PV generator is maximum. During winter, the PV generator reaches a peak power ranging from 0.5 kW to 1.2 kW, depending on the orientation of the modules. As expected, in summer months, PV production is higher, reaching peak values between 1.5 kW and 2 kW. Fig. 6 shows that, in summer, PV production is always higher than the loads, except for the afternoon in Study Room #1 (SE orientation). In such conditions, the BESS is not strictly necessary, while the integration of an optimal storage unit is fundamental in winter and during days with low irradiance. Indeed, during winter, PV production cannot supply the entire demand (Fig. 5). In particular, in case of Study Room #1 and #2, the loads are higher than PV generation and, without the BESS, the absorption from the grid would be relevant. In Table 2, the results of the simulations performed with several batteries capacities are reported:

TABLE II. RESULTS OF THE SIMULATIONS

C_{bat} [kWh]	$E_{PV,yearly}$ [kWh]	$E_{load,yearly}$ [kWh]	R_{suff} [%]	$E_{grid,abs}$ [kWh]
0	8660	3874	61.0	1509
16			84.1	617
20			85.3	570
24			86.3	530
28			86.9	505
32			87.4	488
36			87.8	473

The storage capacity that permits an adequate compromise between high self-sufficiency and low costs is 16 kWh. Indeed, R_{suff} remarkably increases from 61% to 84% thanks to the batteries, but the further growth from 84% to 88% does not justify the higher costs of a larger capacity. Moreover, the absorption from the grid is similar and negligible for all the analyzed configurations and in case of C_{Ebat}= 16 kWh it is equal to 617 kWh. Therefore, the goal of the nZEB in terms of grid absorption is reached and the consumptions are almost supplied by PV production. As shown in Fig. 7, from April to October, the building is completely self-sufficient (R_{suff}=100%) while the minimum value of self-sufficiency is reached in December (R_{suff} =53.3%).

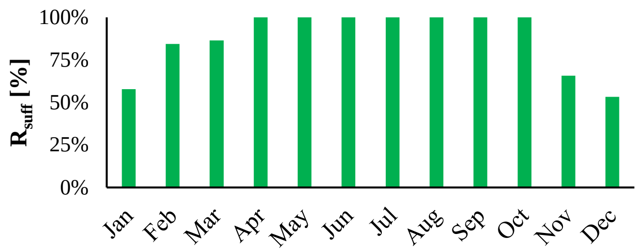

Figure 7. Monthly self-sufficiency of the building.

VI. CONCLUSIONS

The present project shows a case study of a prototype of a prefabricated nZEB for academic purposes. Results demonstrate that the optimal capacity of batteries in the PV-storage system corresponds to C_{bat}=16 kWh, with R_{suff}≈84% and low absorption from the grid ($E_{grid,abs}$≈600 kWh). Moreover, the system reaches high levels of self-sufficiency due to its designated use, leading to the contemporaneity between the PV production and the loads. The total self-sufficiency is achieved for seven months per year (from April to October) and in the worst winter month R_{suff} reaches values higher than 50%. The presented nZEB includes the installation of proper sensors that are smart metering oriented. The future goal will be to achieve the global yearly self-sufficiency. Load flexibility will be taken into account, for example, by reducing the number of available workstations during days with low predicted PV production.

REFERENCES

[1] A. I. Nousdilis *et al.*, "Enhancing storage integration in buildings with photovoltaics (PV-ESTIA project)," in Proc. *2018 IEEE International Energy Conference (ENERGYCON)*, pp. 1-5.

[2] Directive 2010/31/EU of the European Parliament and of the Council, 19 May 2010.

[3] M. Medrano, J.M. Martí, L. Rincón, G. Mor, J. Cipriano, M. Farid, "Assessing the nearly zero-energy building gap in university campuses with a feature extraction methodology applied to a case study in Spain," *International Journal of Energy and Environmental Engineering*, pp.1-21, 2018.

[4] M. H. Chung, E. K. Rhee, "Potential opportunities for energy conservation in existing buildings on university campus: A field survey in Korea," *Energy and Buildings*, vol. 78, pp. 176-182, 2014.

[5] É. Mata, F. López, A. Cuchí, "Optimization of the management of building stocks: An example of the application of managing heating systems in university buildings in Spain," *Energy and Buildings*, vol. 41, pp. 1334-1346, 2009.

[6] M. S. Gul, S. Patidar, "Understanding the energy consumption and occupancy of a multi-purpose academic building," *Energy and Buildings*, vol. 87, pp. 155-165, 2015.

[7] G. Escrivá-Escrivá, "Basic actions to improve energy efficiency in commercial buildings in operation," *Energy and Buildings*, Vol. 43, pp. 3106-3111, 2011.

[8] Wim Zeiler, Gert Boxem, "Net-zero energy building schools," *Renewable Energy*, Vol. 49, 2013, pp. 282-286.

[9] Yang Zhang, Anders Lundblad, Pietro Elia Campana, Jinyue Yan, "Employing Battery Storage to Increase Photovoltaic Self-sufficiency in a Residential Building of Sweden," *Energy Procedia*, Vol. 88, 2016, pp. 455-461.

[10] Luis Ramirez Camargo, Felix Nitsch, Katharina Gruber, Wolfgang Dorner, "Electricity self-sufficiency of single-family houses in Germany and the Czech Republic," *Applied Energy*, Vol. 228, 2018, pp. 902-915.

[11] Sylvain Quoilin, Konstantinos Kavvadias, Arnaud Mercier, Irene Pappone, Andreas Zucker, "Quantifying self-consumption linked to solar home battery systems: Statistical analysis and economic assessment," *Applied Energy*, Vol. 182, 2016, pp. 58-67.

[12] R. Velik "The influence of battery storage size on photovoltaics energy self-consumption for grid-connected residential buildings," Renewable Energy Res, 2013.

[13] L. Wells, B. Rismanchi, L. Aye, "A review of Net Zero Energy Buildings with reflections on the Australian context," *Energy and Buildings*, Vol. 158, pp 616-628, 2018.

[14] M. Gürtürk, H. Benli, N. K. Ertürk, “Effects of different parameters on energy – Exergy and power conversion efficiency of PV modules,” *Renewable and Sustainable Energy Reviews*, vol. 92, pp. 426-439, 2018.

[15] F. Spertino, J. Ahmad, A. Ciocia, P. Di Leo, "How much is the advisable self-sufficiency of aggregated prosumers with photovoltaic-wind power and storage to avoid grid upgrades?," in Proc. *2017 IEEE Industry Applications Society Annual Meeting*, pp. 1-8.

[16] J. M.S. Dias, V. A. F. Costa, “Adsorption heat pumps for heating applications: A review of current state, literature gaps and development challenges,” *Renewable and Sustainable Energy Reviews*, vol. 98, pp. 317-327, 2018.

[17] M. B. Téllez. Molina, M. Prodanovic, "Profitability assessment for self-sufficiency improvement in grid-connected non-residential buildings with on-site PV installations," in Proc. *2013 International Conference on Clean Electrical Power (ICCEP)*, pp. 353-360.

[18] G. Krese, Ž. Lampret, V. Butala, M. Prek, “Determination of a Building's balance point temperature as an energy characteristic,” *Energy*, vol. 165, Part B, pp. 1034-1049, 2018.

[19] F. Spertino, A. Ciocia, P. Di Leo, R. Tommasini, I. Berardone, M. Corrado, A. Infuso, M. Paggi, “A power and energy procedure in operating photovoltaic systems to quantify the losses according to the causes,” Solar Energy, Vol. 118, 2015, pp. 313-326.

[20] F. Spertino, A. Ciocia, F. Corona, P. Di Leo, F. Papandrea, "An experimental procedure to check the performance degradation on-site in grid-connected photovoltaic systems," in Proc. *2014 IEEE 40th Photovoltaic Specialist Conference (PVSC)*, pp. 2600-2604.

[21] M. Muller, B. Marion, J. Rodriguez, “Evaluating the IEC 61215 Ed.3 NMOT procedure against the existing NOCT procedure with PV modules in a side-by-side configuration,” in Proc. *2012 38th IEEE Photovoltaic Specialists Conference*, pp. 697-702.

[22] National Renewable Energy Laboratory, System Advisor Model [Internet]. Available from: https://sam.nrel.gov/ [Accessed: 2018-11-10].

[23] F. Spertino, A. Ciocia, V. Cocina and P. Di Leo, "Renewable sources with storage for cost-effective solutions to supply commercial loads," in Proc. *2016 International Symposium on Power Electronics, Electrical Drives, Automation and Motion (SPEEDAM)*, pp. 242-247.

[24] M. Koller, T. Borsche, A. Ulbig, G. Andersson, “Defining a degradation cost function for optimal control of a battery energy storage system,” in Proc. *2013 IEEE Grenoble Conference*, pp. 1-6.

[25] F. Spertino, J. Ahmad, A. Ciocia, P. Di Leo, “Techniques and Experimental Results for Performance Analysis of Photovoltaic Modules Installed in Buildings”, *Energy Procedia*, vol. 111, pp. 944-95, 2017.